

Sequential application of mineralized electroconductive scaffold and electrical stimulation for efficient osteogenesis

Mohammad Omid Oftadeh,^{1,2} Behnaz Bakhshandeh,¹ Mohammad Mehdi Dehghan,^{3,4} Arash Khojasteh⁵

¹Department of Biotechnology, College of Science, University of Tehran, Tehran, Iran

²Stem Cell Technology Research Center, Tehran, Iran

³Department of Surgery and Radiology, Faculty of Veterinary Medicine, University of Tehran, Tehran, Iran

⁴Institute of Biomedical Research, University of Tehran, Tehran, Iran

⁵Department of Tissue Engineering and Applied Cell Sciences, School of Advanced Technologies in Medicine, Shahid Beheshti University of Medical Sciences, Tehran, Iran

Received 7 August 2017; revised 24 November 2017; accepted 20 December 2017

Published online 11 January 2018 in Wiley Online Library (wileyonlinelibrary.com). DOI: 10.1002/jbm.a.36316

Abstract: Osteogenic differentiation is enhanced by many inductive factors including biochemical agents, biomechanical stresses, and electrical stimulation. Regularly studies have focused on one factor at a time, while synergies can promote more effective and functional osteogenesis. Herein, for the first time, functional synergism between application of electrical stimulation and HA nanoparticles was evaluated in osteogenic differentiation. Prepared electrospun biocompatible conductive scaffold by amalgamating chitosan, aniline-pentamer, and hydroxyapatite incorporation was seeded by human bone-marrow-derived mesenchymal stem cells. The cells seeded on the scaffolds with and without hydroxyapatite were exposed to electrical stimulation and subsequently, osteogenic molecular markers and related signaling pathways were investigated. In general, all investigated osteogenic markers (osteocalcin, alkaline phosphatase, osteonectin, and Runx2) were upregulated transcriptionally in the cells seeded on the chitosan-embedded

scaffolds. Separate utilization of electrical stimulation or hydroxyapatite-enhanced osteogenesis, while the cells exposed to both stimulators simultaneously, expressed higher levels of some of osteogenic genes significantly. Considering the functions and the positions of the markers in osteogenic signaling pathways, it can be concluded that HA might cooperate in the allocation of stem cells to osteoprogenitors in the early phase of osteogenesis while electrical stimulation helps committed cells with maturation and acquiring functional phenotypes. Altogether investigation of the synergism between different stimulators and exploiting the interactions in an optimized manner could lead to more efficient osteogenesis protocol for effective bone regeneration and tissue engineering. © 2018 Wiley Periodicals, Inc. *J Biomed Mater Res Part A*: 106A: 1200–1210, 2018.

Key Words: bone tissue engineering, electrical stimulation, hydroxyapatite, conductive polymer, stem cell

How to cite this article: Oftadeh MO, Bakhshandeh B, Dehghan MM, Khojasteh A. 2018. Sequential application of mineralized electroconductive scaffold and electrical stimulation for efficient osteogenesis. *J Biomed Mater Res Part A* 2018;106A:1200–1210.

INTRODUCTION

Tissue engineering has been recently introduced as a promising strategy for tissue repair and replacement. Although bone has remodeling capability, healing nonunion fractures and huge defects remains problematic. Hence, bone tissue engineering with appropriate cell type, osteoconductive agents, and biocompatible materials is under focus.¹

Demonstration of piezoelectric properties of bone by Fukada and Yasuda² inspired researchers to exploit electrical stimulation for osteogenesis procedure. Previously, direct stimulation, capacitive-coupling, and inductive-coupling methods were utilized to deliver electrical stimulus with dissimilar effects on osteoblasts and mesenchymal stem cells.³ Capacitive-coupling enhanced proliferation, extracellular matrix (ECM) deposition alkaline phosphatase activity,

bone-morphogenetic protein 2 (BMP-2) expression, and ventricular endothelial growth factor (VEGF) improvement. On the other hand, inductive-coupling inhibited cell growth and enhanced mineralization and expression of BMP-2 and transforming growth factor beta 1 (TGFβ-1).³ Besides, implementation of direct stimulation enhanced the expression of osteogenic factors particularly BMP-2, BMP-6 and BMP-7.^{4,5} However, the use of electro-conductive polymeric scaffolds was a breakthrough in this field.⁶ Electrical conductivity mimics electrical properties of bone matrix that caused by collagen proteins naturally.^{7–13}

Among conductive polymers, polypyrrole, polyaniline, and polythiophenes have been extensively utilized in biomedical engineering as biosensors, neural probes, tissue engineering scaffolds, drug delivery carriers, and so on.^{14,15} Polyaniline

Correspondence to: B. Bakhshandeh; e-mail: b.bakhshandeh@ut.ac.ir

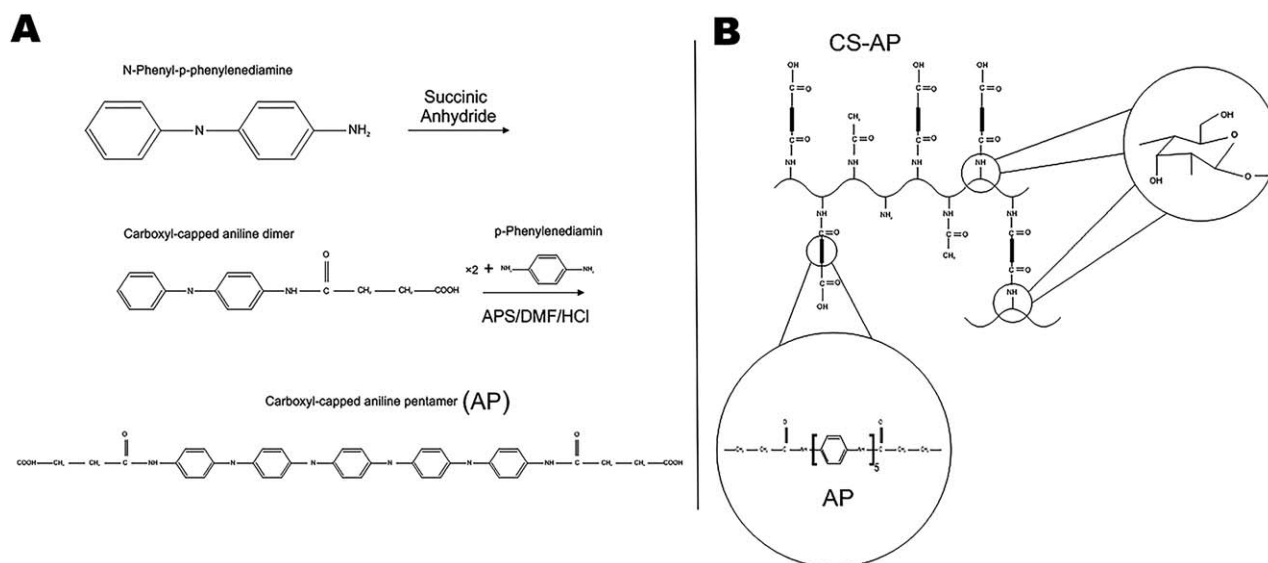


FIGURE 1. Schematic representation of (A) aniline pentamer (AP) and (B) chitosan-grafted-aniline pentamer (AP) syntheses.

has many advantages such as proper environmental stability, low expense, and ease of synthesis.^{16–18} On the other hand, several disadvantages such as nonbiodegradability, low flexibility, and difficulty of processing limit its application.^{19,20} To overcome the problem of nonbiodegradability, application of oligomers instead of polymers has been proposed due to the consumption and elimination of oligomers by macrophages.²¹ Aniline pentamer (AP, an oligoaniline) shows the electrical properties similar to polyaniline with more flexibility in processing and biodegradability.^{22,23}

Blending conductive polymers with conventional biocompatible polymers is another approach to enhance biocompatibility and biodegradability.^{12,22–24} Chitosan (a natural polymer) has been widely used in bone engineering because of its biocompatibility, biodegradability, similarity to glycosaminoglycans (the main components of bone ECM) and the capability to enhance osteogenesis.^{25–30}

Hydroxyapatite (HA), as another natural material, is also incorporated in scaffolds to mimic mineralized ECM of bone for osteogenesis improvement.^{31–34} In addition to improvement of osteoinductivity, osteoconductivity, and cell viability, exploitation of HA boosts mechanical strength of the scaffolds.^{31,35,36}

Regularly studies have focused on one factor at a time, while the synergies can be probably exploited to promote more effective and functional osteogenesis. In this research, to the best of our knowledge for the first time, the functional synergism of two osteoconductive factors (HA and electrical stimulation) in osteogenic differentiation was investigated. In other words, we examine the hypothesis that applying HA and electrical stimulation simultaneously to the cells would further promote osteogenic differentiation than individual stimulators.

Due to the capability of self-renewal and differentiation into different lineages³⁷ and also, because of the potential for patient-specific therapy,³⁸ hBM-MSCs were selected for this

study. Previous study stated that electrical stimulation, when applied to MSCs, improved proliferation, TGFβ-1 expression, alkaline phosphatase activity, and ECM mineralization.³ Kim et al. indicated that VEGF expression increased in MSCs only when biphasic electric current stimulation was applied.³⁹ Titushkin et al. showed alteration in biomechanical properties of MSCs in response to electrical stimulation⁴⁰ and Sun et al. reported that MSCs migrated toward cathode in an electrical field (galvanotaxis).⁴¹

Aniline pentamer is a sequence of five aniline monomers (a phenyl group attached to an amine group) bounded to each other by their amine groups. Hu et al. synthesized aniline pentamer coupled with chitosan and showed its biocompatibility.²² Recently, Liu et al. constructed aniline pentamer-graft-gelatin/PLLA nanofibers using electrospinning for bone tissue engineering purposes.⁴²

MATERIALS AND METHODS

Materials

Dulbecco Modified Eagle's Medium (DMEM), fetal bovine serum (FBS) and trypsin enzyme were purchased from Gibco, Germany. MTT solution (3-(4, 5-dimethylthiazol-2-yl)-2, 5-diphenyltetrazolium bromide), dimethyl sulfoxide (DMSO), succinic anhydride, dimethyl formamide (DMF), N-hydroxysuccinimide (NHS), 1-ethyl-3-(3-dimethylaminopropyl) carbodiimide (EDC), N-phenyl-p-phenylenediamine, p-phenylenediamine, hydrochloric acid (HCl), PEO (400,000 Da), and HA (particle size < 200 nm) were purchased from Sigma-Aldrich, USA. Low-viscosity chitosan was purchased from Fluka, USA.

Syntheses of aniline pentamer (AP) and chitosan grafted-aniline pentamer (CS-AP)

As illustrated in Figure 1, the syntheses of AP and CS-AP were carried out according to the previous reports.^{22,43} Briefly, to synthesize AP, N-phenyl-p-phenylenediamine and

succinic anhydride reacted to obtain phenyl/carboxyl-capped aniline dimer. The resulted phenyl/carboxyl-capped aniline dimer and p-phenylenediamine were dissolved in HCl/DMF and ammonium persulfate was added to reach emeraldine base form of AP. Finally, emeraldine base were fully reduced to achieve leucoemeraldine using ammonia solution (NH₄OH). For the synthesis of CS-AP, NHS-capped AP was produced in the following way: AP (3.3 mmol), NHS (11.3 mmol), and EDC (15.1 mmol) were dissolved in 20 mL DMF at stirring condition for overnight. Then the mixture was filtered and the solvent was allowed to dry out. The remaining precipitate was dissolved in DMF so that the final concentration of NHS-capped AP was 1% wt. Thereafter, chitosan (1% wt) was dissolved in 50 mL aqueous acetic acid solution (50% wt) supplemented with 2 mL DMSO and subsequently, 10 mL of the prepared solution of NHS-capped AP in DMF was added gradually to reach the CS-AP (2% wt) as final concentration.

Fabrication of nanofibrous scaffold

Solutions of PEO and CS-AP were prepared by dissolving them separately in aqueous 50% wt acetic acid under magnetic stirring overnight. The concentration of PEO and CS-AP solutions were 5% and 2% wt, respectively. Then, the solutions of PEO and CS-AP were mixed so that the mass ratio of CS-AP to PEO was 1:1 in the final solution. To provide HA suspension, mixture of 5% wt HA and aqueous acetic acid solution (50% wt) was prepared and stirred for 10 min. Then the mixture was sonicated subsequently for 10 min to achieve better dispersion. Afterward, the HA suspension was added to PEO/CS-AP solution so that the ratio of HA to the polymers was 1:8 in the final mixture. After 10 min stirring, the final mixture was sonicated for 10 min before electrospinning.

The electrospinning parameters were the same for both scaffolds (with HA (CS-AP-HA) and without HA (CS-AP)). The fibers were attained with the following adjustment: 20 kV voltage, 0.3 mL/h flow rate, and 20 cm distance between nozzle and collector. Ten-milliliter syringes and aluminum rotating drum with 300 rpm rotating speed were used.

Scaffold characterization

Scanning electron microscopy. The morphology and structure of CS-AP and CS-AP-HA scaffolds were characterized using Scanning Electron Microscopy (SEM) (HITACHI S-4160, Japan). Samples were coated with gold by sputter coater.

FTIR spectroscopy. To scrutinize the synthesis of CS-AP, FTIR spectrum of powder of the final product was recorded and analyzed. In addition, FTIR spectroscopy (Bruker, Germany) was performed after fabrication of scaffolds, either with or without HA, to investigate HA incorporation.

Contact angle measurement. To measure static apparent contact angle and hydrophilicity, a droplet of water (10 μ l) was placed on each scaffold and studied using a homemade telescope goniometer mounted with a CCD camera.

Tensile strength. For mechanical strength evaluation, tensile test was performed using a tensile tester (SANTAM Stress machine STM20, Iran). To perform the test, rectangular samples³⁵ with dimensions of 40 \times 10 mm² and thickness of 10 μ m were cut from CS-AP and CS-AP-HA scaffolds. The test was performed at room temperature and 10 mm/min speed with 200 N as load cell.

Cyclic voltammetry. In addition, cyclic voltammetry (CV) was implemented to study electrochemistry of both CS-AP and CS-AP-HA scaffolds using HCl as the supporting electrolyte. Silver chloride electrode was used as reference electrode. Autolab PGSTAT128N device and NOVO software were utilized for this test.

Isolation, expansion, and characterization of hBM-MSCs

hBM-MSCs were isolated and characterized according to the protocols that described previously.⁴⁴ Briefly, after bone marrow aspirate obtaining from the posterior iliac crest, aspirate diluted with DMEM (3:1 ratio) and on the next day, nonadherent components were eliminated by discarding the medium. The samples were obtained from different voluntary donors (Taleghani Hospital, Tehran, Iran) with signed letters of consent based on Iran's Ministry of Health Medical Ethics Committee guidelines. Fresh DMEM containing FBS (10% v/v), 100 unit/ml penicillin, and 100 μ g/ml streptomycin was used for culture. The samples were stored in an incubator with humidified atmosphere containing 5% CO₂ at 37°C. Each time, the cells reach favorable confluency, and subcultures were provided.

CD markers of this cell type were investigated as reported previously.³⁸ Briefly, the cells were stained with monoclonal antibodies against human CD34, CD44, CD90, CD105 (all FITC-conjugated), CD73, and CD166 (both PE-conjugated) (all from Dako, Glostrup, Denmark). In every test, the suitable isotype matched antibody was used as control to cover nonspecific binding. Flow cytometry analysis was performed on FACS Calibur cytometer (Becton Dickinson) using CellQuest software. Win MDI 2.8 software was used to create the histograms.

Cell seeding

Disk-shape scaffolds with 3 cm diameter and 2 μ m thickness were prepared to match 6-well plates of the bioreactor used for electrical stimulation. Before seeding, the samples were sterilized with 70% ethanol and ultraviolet (UV) exposure for 30 min. The UV light intensity was 30 μ W/cm²; no chemical change is occurred in the scaffold at this light intensity.⁴⁵ Then the samples were swamped with DMEM containing FBS (10% v/v) and incubated overnight to facilitate cell attachment. The hBM-MSCs (passages 2–4) were seeded onto the scaffolds with initial density of 5 \times 10⁴ cells/well.⁴⁶

Cell viability

To assess the cell viability of the scaffolds (CS-AP and CS-AP-HA), MTT assay was performed. The scaffolds were cut into disk shapes that fit into 96-well plate. hBM-MSCs with

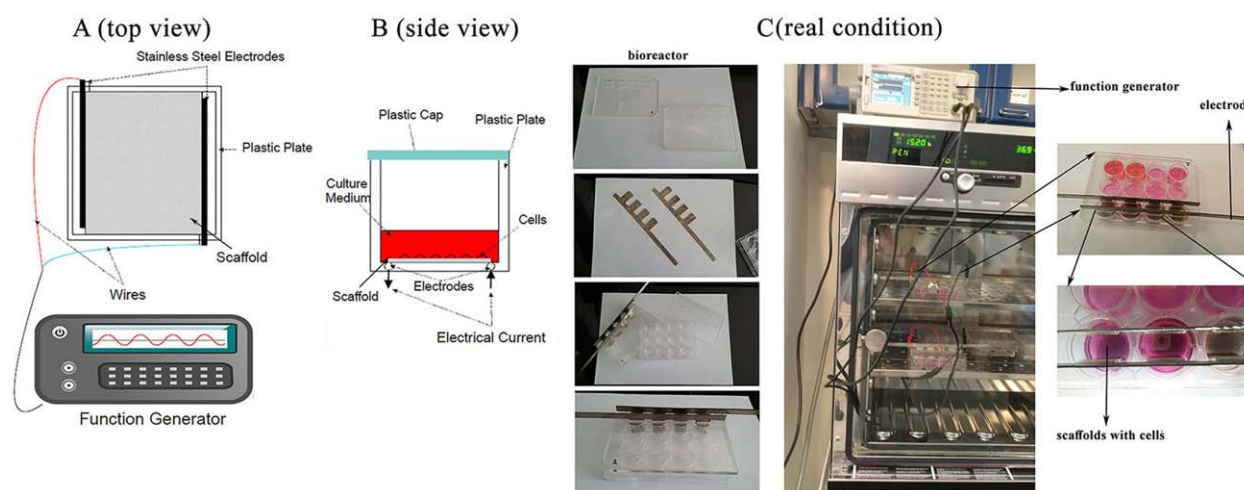


FIGURE 2. Schematic representation of (A) the top view and (B) the side view of the bioreactor and (C) the real condition and equipment in the experiment.

3×10^3 cells/well density, were seeded into each well. On days 1, 3, 7, and 14 ($n = 3$ for each day), the media of wells were discarded and 150 μ L of culture medium containing 10% MTT solution (5 mg/mL) (alfa aesar, China) was added to each well. After incubation for 3 h, MTT solution was discarded and 150 μ L of DMSO was added. The optical density was read after removing the scaffolds at a wavelength of 570 nm by spectrophotometer (BioTek Instruments, USA). Data were presented as percentage ratios of test group absorbance over control group absorbance. Six-hours culture was considered as control group.

Electrical stimulation

The electrical stimulation was commenced two days after cell seeding. To deliver electrical stimuli, the bioreactor described in the previous study⁴⁷ was used (Fig. 2). In opposite sides of the bottom of each well of the bioreactor, two stainless steel electrodes^{48,49} were placed. The conductive scaffolds were placed on the top of the electrodes and in contact with them. The electrical signal was generated by a function/arbitrary waveform generator (GPS, GPS-2105, UK) and delivered through two wires that were connected to the opposite electrodes. The electrical setup was adjusted according to previous studies.^{9,46} Each well experienced an electrical signal with a 2 V voltage and 100 Hz frequency for 2 h/day for 7 and 14 days. According to the previous reports,^{46,50} 100 Hz electrical stimulation showed no significant cytotoxicity.

Calcium content and alkaline phosphatase (ALP) activity assays

Calcium content of the samples on days 7 and 14 was assessed by Arsenazo III kit (Parsazmun, Iran). The samples were treated with 0.6 N HCl and shaken for 4 h at 4°C. Subsequently, the reagents were added and the absorbance was read at 630 nm for each sample. To quantify the calcium content, the results were compared with standard curve.

In addition, for cultures of days 7 and 14, ALP activity of the samples was measured by assessing p-nitrophenyl

phosphate hydrolysis kinetics in the presence of ALP. After extracting total protein using RIPA buffer, cell debris were sedimented by centrifugation at 15 000 rpm and 4°C for 15 min. The supernatant was collected and assessed by an ALP activity assay kit (Parsazmun, Iran) at 405 nm. Finally, enzyme activity (IU/L) was normalized against total protein concentration (mg/L) in each sample.

Transcriptional analyses

After 7 and 14 days, osteogenic marker genes (Table I) were evaluated quantitatively in the cells cultured on either CS-AP or CS-AP-HA and either with or without electrical stimulation ($n = 3$ for each group). The seeded cells on the tissue culture polystyrene (TCPS) were considered as the control group. Total RNA extraction was performed by phenol-chloroform extraction procedure. Cell lysis was performed by RNX-Plus lysis buffer (Sinaclone, Iran) and the lysate was collected using centrifugation at 4°C and 12,000 rpm for 15 min. After cDNA synthesis, the target genes were evaluated by real-time PCR machine (Corbett, Australia). The results were analyzed by $\Delta\Delta C_t$ method and normalized against GAPDH (as the internal control gene^{12,46}). All enzymes, buffers, and agents for real-time PCR were purchased from Vivantis (Malaysia).

TABLE I. The Sequences of the Primers for Real-Time PCR Analyses

Genes	Primer Sequences
GAPDH	ACTTTGTCAAGCTCATTTC (F) TGCAGCGAAGTTTATTGATG (R)
RUNX2	GCCTTCAAGGTGGTAGCCC (F) CGTTACCGCCATGACAGTA (R)
OSTEOCALCIN (OC)	GCAAAGGTGCAGCCTTTGTG (F) GGCTCCCAGCCATTGATACAG (R)
OSTEONECTIN (ON)	AGGTATCTGTGGGAGCTAATC (F) ATTGCTGCACACCTTCTC (R)
ALKALINE PHOSPHATASE (ALP)	ATGTCTGGAACCGCACTGAA (F) CGCCTGGTAGTTGTTGTGAGCATAG (R)

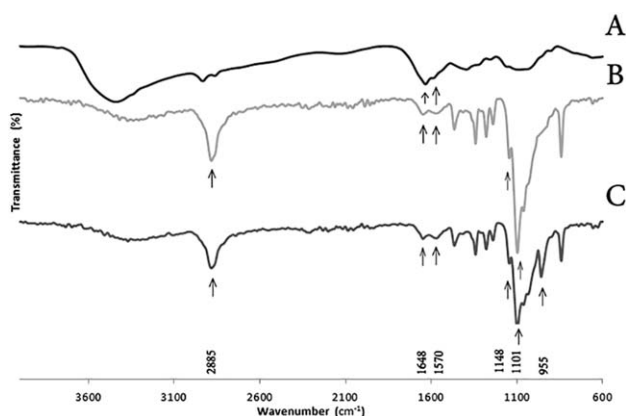


FIGURE 3. FTIR spectra of (A) chitosan-grafted-aniline pentamer, (B) chitosan-grafted-aniline pentamer/poly ethylene oxide (CS-AP), and (C) chitosan-grafted-aniline pentamer/poly ethylene oxide/hydroxyapatite (CS-AP-HA).

Statistical analysis

All statistical analyses were performed by SPSS (version 13.0, US) using one-way analysis of variance (ANOVA). The difference was considered statistically significant at $p < 0.05$ or $p < 0.01$ and data were illustrated as mean \pm standard deviation (SD). All experiments were done in triplicate, unless otherwise stated.

RESULTS

Production of mineralized electroactive biopolymer

Evaluation of synthesized AP and CS-AP. According to the FTIR spectrum [Fig. 3(A)], characteristic peaks of CS-AP,^{24,51} including a peak at 1647 cm^{-1} (corresponding to C=O stretching vibration) from chitosan and a peak at

1570 cm^{-1} (corresponding to quinoid ring) from AP, were detected. Remarkably, the absence of a peak at about 1718 cm^{-1} , appearing in the AP spectrum and corresponding to COOH group, proved the synthesis of CS-AP.

Characterization of mineralized electroactive biopolymer. FTIR spectroscopy indicated the presence of HA in the final CS-AP-HA nanofibrous mat [Fig. 3(B,C)]. Comparing FTIR spectra of CS-AP-HA and CS-AP showed the presence of a new peak at 955 cm^{-1} , corresponding to the stretching vibration band of P—O in PO_4^{3-} from HA.³⁶ Furthermore, two new peaks at 1101 cm^{-1} and 1148 cm^{-1} (corresponding to C—O—C stretching vibration) and a new peak at 2885 cm^{-1} (corresponding to methylene group),⁵² appeared in CS-AP and CS-AP-HA spectra with respect to the spectrum of CS-AP, confirmed the presence of PEO in the electrospun nanofibers of both scaffolds.

The SEM images illustrated that the nanofiber diameter was $\sim 200\text{ nm}$ in both CS-AP and CS-AP-HA scaffolds [Fig. 4(A,C)].

The mechanical strengths of CS-AP and CS-AP-HA scaffolds were determined by tensile test to evaluate the Young's modulus. Based on the curves [Fig. 5(A)] and calculated Young's modules (Table II), CS-AP elongated fairly quickly while pressure was increased gradually; when the sample broke under 2.5 MPa , it had elongated $\sim 23\%$. On the other hand, the tensile stress on CS-AP-HA increased rapidly to reach 11.9 MPa at maximum while elongation was $\sim 6\%$.

As water contact angles were $< 90^\circ$ in CS-AP and CS-AP-HA scaffolds (i.e., 34° and 46° , respectively), the mentioned scaffolds were considered hydrophilic; the incorporation of HA increased contact angle slightly [Fig. 5(B)].

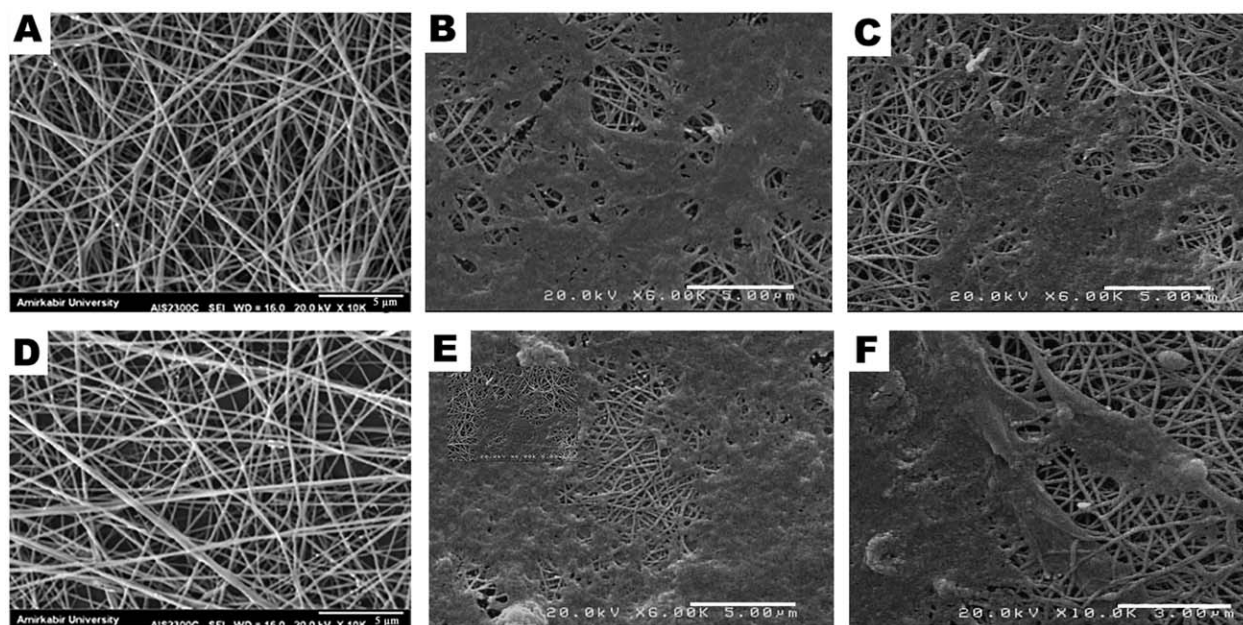


FIGURE 4. SEM images of chitosan-grafted-aniline pentamer/poly ethylene oxide (CS-AP) (A) without cells, (B) with cells, and (C) under electrical stimulation; chitosan-grafted-aniline pentamer/poly ethylene oxide/hydroxyapatite (CS-AP-HA) (D) without cells, (E) with cells, and (F) under electrical stimulation.

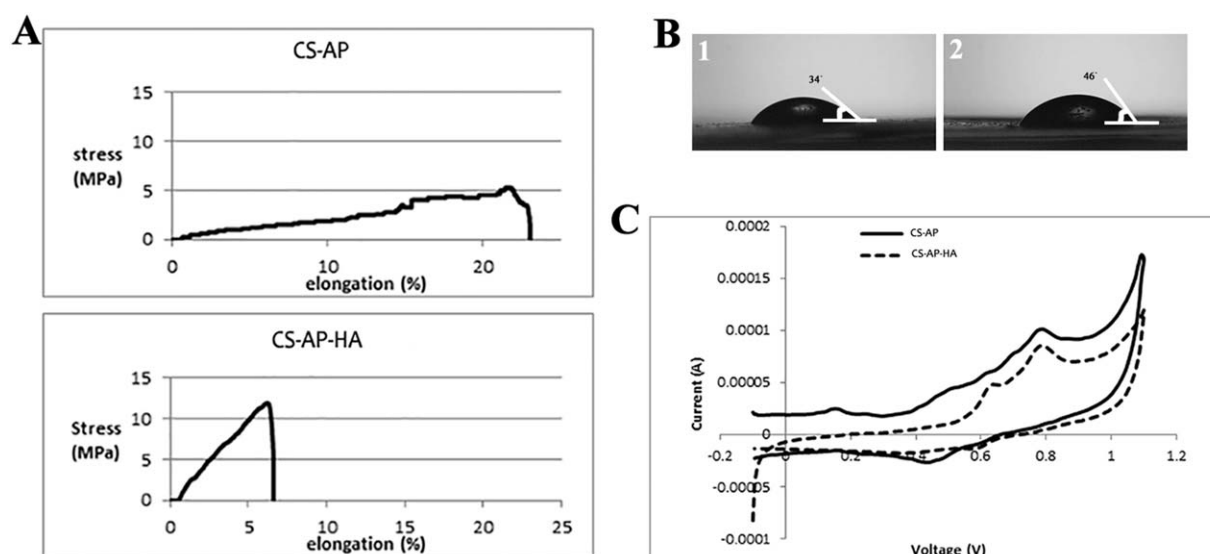


FIGURE 5. (A) Stress-strain curves for chitosan-grafted-aniline pentamer/poly ethylene oxide (CS-AP) and chitosan-grafted-aniline pentamer/polyethylene oxide/hydroxyapatite (CS-AP-HA), (B) static contact angle measurement for CS-AP (1) and CS-AP-HA (2), and (C) cyclic voltammetry curves for chitosan-grafted-aniline pentamer/polyethylene oxide (CS-AP) and chitosan-grafted-aniline pentamer/polyethylene oxide/hydroxyapatite (CS-AP-HA).

Electrochemical properties of CS-AP and CS-AP-HA scaffolds were studied by CV analysis [Fig. 5(C)]. The mean peak potentials ($E_{1/2} = \frac{E_{pa} + E_{pc}}{2}$) were 0.47, 0.61, and 0.81 V for three peaks of CS-AP, respectively. On the other hand, only two peaks could be distinguished in CS-AP-HA diagram with mean peak potentials that were, respectively, 0.61 and 0.79 V.

Cell viability evaluation of the scaffolds. MTT assay was carried out to evaluate the cell viability of the scaffolds. The ratios of cell proliferation on CS-AP or CS-AP-HA scaffolds in comparison to TCPS were higher than 95% confirming that neither of the scaffolds was cytotoxic (Fig. 6). As shown, after a decrease from day 1 to day 3, the number of viable cells increased steadily on both scaffolds from day 3 to day 14. Although the rate of cell proliferation was higher on the CS-AP-HA scaffold compared to the CS-AP scaffold, statistical analysis showed no significant difference.

Osteogenic differentiation by sequential application of mineralized electroactive biopolymer and electrical stimulation

ALP activity upregulated significantly in the presenting HA. Also, electrical stimulation enhanced ALP activity in 7th and 14th day of culture. However, ALP activity in cells cultured

on CS-AP was not significantly different from control group (TCPS) whether in the absence or presence of electrical stimulation [Fig. 7(A)]. Similarly, both electrical stimulation and HA enhanced calcium deposition, while the effect of HA can be identified earlier than electrical stimulation [Fig. 7(B)].

Some gene markers were investigated during osteogenic differentiation of hBM-MSCs under electrical stimulation (Figs. 2 and 8). Prior to this evaluation, the CD markers of the cells were investigated by flow cytometry. As previously reported, they expressed CD34 while the cells were negative for CD44, CD90, CD105, CD73, and CD166.³⁸

Overall, all investigated osteogenic markers (alkaline phosphatase (ALP), osteocalcin, osteonectin, and Runx2) were upregulated transcriptionally in the cells seeded on the chitosan embedded scaffolds in comparison to TCPS (tissue culture polystyrene as control group). Separate utilization of electrical stimulation or hydroxyapatite enhanced osteogenesis, while the cells exposed to both stimulators simultaneously, expressed higher levels of some of osteogenic genes significantly. Considering all test groups, on day 7, ALP transcription on CS-AP-HA (without electrical stimulation) was significantly higher than the other groups. Prolonged electrical stimulation in combination with HA exposure caused significant upregulations in ALP

TABLE II. Mechanical Properties of Chitosan-Grafted-Aniline Pentamer/Polyethylene Oxide (CS-AP) and Chitosan-Grafted-Aniline Pentamer/Polyethylene Oxide/Hydroxyapatite (CS-AP-HA)

	Young's Modules (MPa)	Ultimate Stress (MPa)	Breakage Stress (MPa)	Ultimate Strain (%)	Breakage Strain (%)
CS-AP	109.92 ± 5.32	5.5 ± 0.31	2.80 ± 0.30	22.98 ± 1.16	23.96 ± 1.01
CS-AP-HA	291.05 ± 9.25	14.32 ± 2.42	12.02 ± 1.22	6.87 ± 0.62	7.33 ± 0.96

In the first column, Young's module is the ratio of tensile stress to tensile strain in the linear part of stress-strain curve.

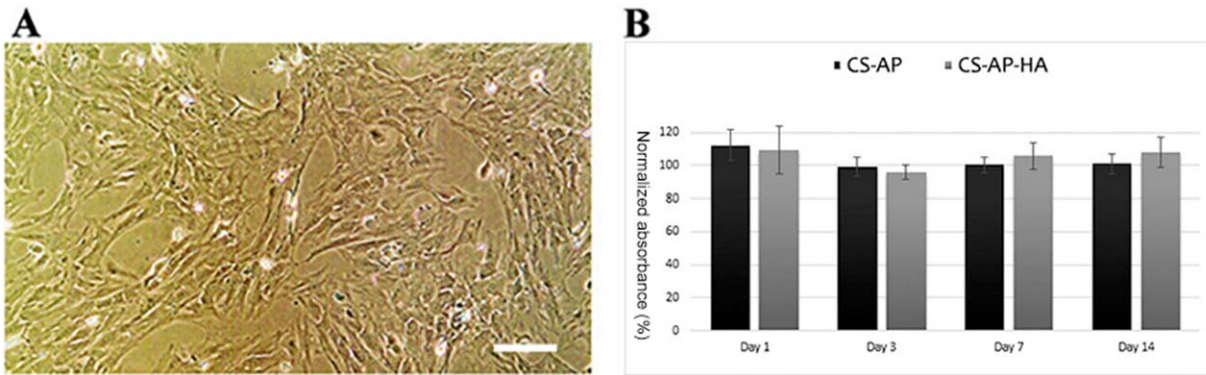


FIGURE 6. (A) phase-contrast microscopy of the hBM-MSC cultured in the polystyrene flask (40 \times magnification) and (B) MTT results for chitosan-grafted-aniline pentamer/polyethylene oxide (CS-AP) and chitosan-grafted-aniline pentamer/polyethylene oxide/hydroxyapatite (CS-AP-HA). Data of vertical axis were presented as percentage ratios of test group absorbance over control group absorbance. Six-hours culture was considered as control group (TCPS). Data are shown as mean \pm standard deviation. Bars: 100 μ m.

transcription on day 14. In both time points, in all test groups (whether undergoing electrical stimulation or not), the transcriptional level of osteocalcin was significantly lower on TCPS than the others. Also, application of HA and electrical stimulation resulted in significant osteocalcin upregulations compared to TCPS. Osteonectin transcription assessment showed significant upregulations under electrical stimulation and HA exposure in both time points and all test groups.

DISCUSSION

Biomineralized scaffolds and electrical stimulation are the two novel stimulators for osteogenic differentiation.⁸ In this research, we attempted to evaluate their possible functional synergism for bone tissue engineering. So, we examine the applicability of electrospun aniline pentamer cross-linking chitosan scaffold for bone tissue engineering. To the best of our knowledge, this is the first study that has utilized

aniline pentamer cross-linking chitosan scaffold as a substrate to apply electrical stimulation to the cells for differentiation. Besides, the synergism between applying hydroxyapatite and electrical stimulation as osteoconductive tools has not been investigated previously.

To achieve this goal, electroconductive scaffolds were prepared using AP as conductive component and HA for biomineralization. Due to insufficient biocompatibility of AP,²⁴ chitosan was supplemented to the scaffold. After AP synthesis, chitosan and AP were coupled chemically (Fig. 1). FTIR spectra of electrospun scaffolds represented the presence of the aforementioned materials, as their characteristic peaks^{36,52} were distinguishable (Fig. 3).

To obtain controllable interconnected porosity, the scaffold was constructed by electrospinning.³¹ Owing to chitosan great positive charge, nonflexible chemical structure, and interference of its specific interactions,^{52–54} PEO was added to the other components to facilitate chitosan

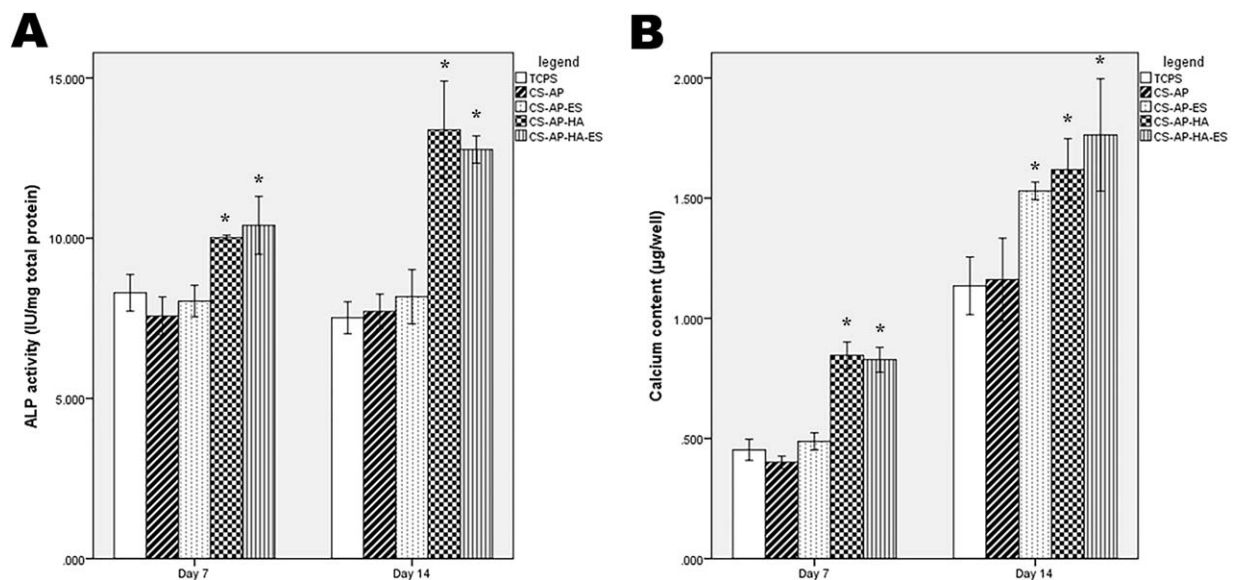


FIGURE 7. Alkaline phosphatase activity (A) and calcium content (B) assays on 7th and 14th day of cell culture. All data shown as mean \pm standard deviation (* p < 0.05).

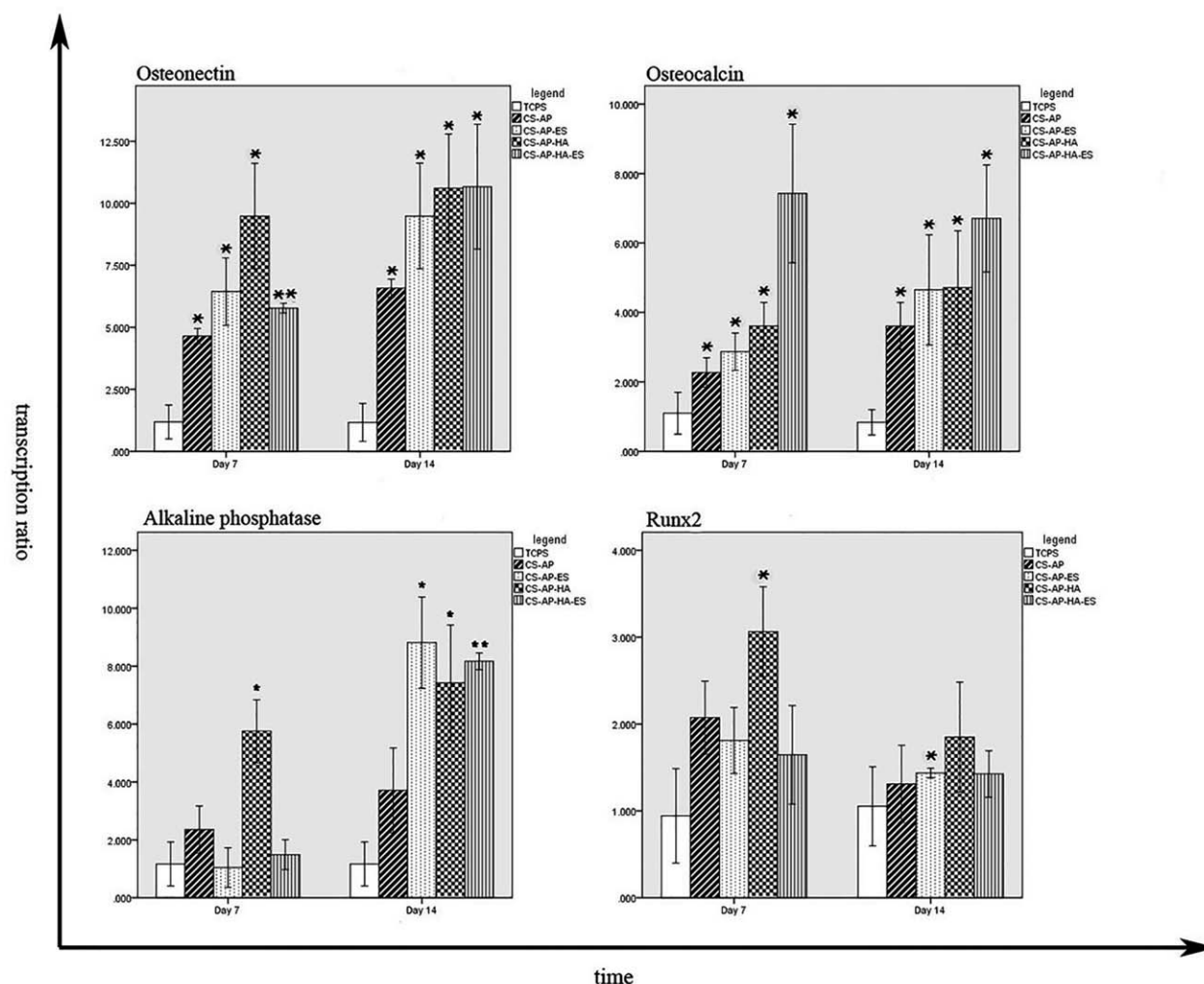


FIGURE 8. Gene transcription level for alkaline phosphatase (ALP), osteocalcin (OC), Runx2, and osteonectin (ON). TCPS: tissue culture polystyrene, CS-AP: chitosan-grafted-aniline pentamer/polyethylene oxide, CS-AP-ES: chitosan-grafted-aniline pentamer/polyethylene oxide with electrical stimulation, CS-AP-HA: chitosan-grafted-aniline pentamer/polyethylene oxide/hydroxyapatite, CS-AP-HA-ES: chitosan-grafted-aniline pentamer/polyethylene oxide/hydroxyapatite with electrical stimulation. All data shown as mean \pm standard deviation (* $p < 0.05$, ** $p < 0.01$).

electrospinning.⁵⁴ SEM images presented the nanofibrous structure with nanoscale size pores (Fig. 4).

As osteogenic differentiation is induced by stiffer matrices,⁵⁵ mechanical stiffness of the scaffold plays major role in specifying stem cells commitment toward osteoblasts. Application of pure chitosan is not appropriate for bone tissue engineering. AP exploitation to chitosan further decreases chitosan mechanical strength²⁴ while the incorporation of HA improves the scaffold mechanical properties.⁵⁶ Tensile test upholds that HA incorporation into CS-AP-HA caused more stiffness and less elasticity and consequently, mechanical strength of scaffold has increased.

In previous works,^{22,43} three peaks were reported for CV curve of CS-AP. The mentioned peaks were observed in CS-AP diagram while only two peaks could be distinguished in CV curve of CS-AP-HA scaffold. It could be explained by the short and weak peaks in the diagram of CS-AP-HA scaffold, and therefore the possible unrecognition of the third peak. Cyclic voltammetry results of CS-AP and CS-AP-HA

scaffolds were comparable with previous reports.^{22,43} CV diagrams for the scaffolds prove that the scaffolds maintain their conductivity even after incorporation of other materials, while incorporation of another nonconductive component, PEO, smoothed the peaks.

MTT assay was carried out to scrutinize the cell viability on CS-AP and CS-AP-HA scaffolds. Based on the results (Fig. 6), the scaffolds did not show significant cytotoxicity during 14 days in comparison to TCPS. According to several reports, HA incorporation enhanced cell proliferation.^{36,57} However, we observed no significant difference between cell population on CS-AP and CS-AP-HA.

Electrical stimulation has been acknowledged as an osteoconductive factor that might have diverse consequences such as TGF β -1 or VEGF upregulation, cell proliferation enhancement, ALP activity improvement, and so forth,³ according to the mechanism of stimulation delivery (e.g., capacitive or inductive) and electrical parameters (e.g., voltage or frequency). Herein we investigated the influence of

electrical stimulation on osteogenic differentiation of hBM-MSCs seeded on CS-AP or CS-AP-HA scaffolds. Also for the first time, the synergism between simultaneous utilization of electrical stimulation and HA was assessed. The osteogenesis was measured by transcription level of several marker genes including ALP, osteocalcin, Runx2, and osteonectin.

The bioreactor and the electrical setup were utilized according to the previous reports.^{46,47} Although the electrodes were not completely isolated from the medium, the presence of scaffolds on the electrodes interferes with physical contact between the electrodes and the medium. More importantly, the main reason for electrochemical corrosion is ionic exchange between the electrode and the medium which entails current passing through medium. However, only 1% of the total current passes through medium and the remaining passes through scaffolds.¹² This is an important advantage for using conductive scaffolds over direct stimulation. In addition, we did not observe any evidence for electrode corrosion at the end of the process.

Enhancement of ALP activity and calcium deposition by applying electrical stimulation and HA was demonstrated in the previous works.^{12,58–60} In this work, calcium deposition and ALP activity were enhanced by exploiting HA, whereas electrical stimulation caused slightly more calcium deposition and ALP activity when applied in combination with HA (Fig. 7).

While HA incorporation caused transcriptional upregulation in the osteogenic marker genes (that is, ALP, osteonectin, and osteocalcin) on early days, ES came into effect on later days and even downregulated some of mentioned genes on day 7 (Fig. 8). These findings were in accordance with previous reports using either HA or electrical stimulation for osteogenic differentiation, respectively.^{10,12,49,57,61} Besides, co-application of HA and ES resulted in the highest upregulation in ALP and osteonectin ($p < 0.01$). However, according to the results, Runx2 gene behaved differently. Our results were corroborated by previous observations as HA incorporation caused increase of Runx2 expression level in the first week after initiation of differentiation and then decreased of Runx2 expression level in the second week,⁵⁷ whereas electrical stimulation could bring about significant growth in Runx2 expression level only in the second week.⁵⁸

Runx2 is an early-stage osteogenic differentiation marker and its expression level increases after the commitment of multipotent stem cells into osteoprogenitor cells.⁶² On the other hand, mineralization (a phenotypic characteristics of osteoblasts) is accomplished by an enzymatic method where ALP is utilized to liberate phosphate ions from organic phosphate compounds.⁶³ Osteonectin (noncollagenous proteins) is also secreted into the mineralized extracellular matrix of osteoblasts.⁶⁴ Considering the functions and positions of the markers in osteogenic signaling pathways,^{65–67} it can be concluded that HA might cooperate in the allocation of stem cells to osteoprogenitors in the early phase of osteogenesis while electrical stimulation helps committed cells with maturation and acquiring functional phenotypes.

CONCLUSION

Osteogenic differentiation is enhanced by many inductive factors including biochemical agents, biomechanical stresses, and electrical stimuli. Most of the researches have focused on one factor at a time, while the synergies can be probably exploited to promote more effective and functional osteogenesis. Herein, for the first time, functional synergism between exploiting electrical stimulation and HA nanoparticles was evaluated for osteogenic differentiation. Separate utilization of electrical stimulation or hydroxyapatite enhanced osteogenesis, while the cells, exposed to both stimulators simultaneously, expressed higher levels of some of osteogenic genes significantly. Taking all the results into account, it could be concluded that co-application of HA and electrical stimulation would further improve osteogenesis as they interfere in the mineralization and osteogenesis signaling pathways sequentially. Altogether investigation of the functional synergism between different stimulators and inspection of the interactions in an optimized manner could lead to more efficient osteogenesis protocol for effective bone regeneration and tissue engineering.

CONFLICT OF INTEREST STATEMENT

The authors have no conflicts of interest.

ACKNOWLEDGMENT

The authors appreciate Dr Nasser Masoumi, Dr Frashid Chini, Dr Mohammad Massumi, Dr Laleh Mahmoudi, Ms Masoumeh-Suri, Mr Alireza Maghsoumi, Stem Cell Technology Research Center and Science & Technology Park of University of Tehran for their kind contributions.

REFERENCES

1. Sadeghi M, Bakhshandeh B, Dehghan MM, Mehrnia MR, Khojasteh A. Functional synergy of anti-mir221 and nanohydroxyapatite scaffold in bone tissue engineering of rat skull. *J Mater Sci Mater Med* 2016;27:132.
2. Fukada E, Yasuda I. On the piezoelectric effect of bone. *J Phys Soc Jpn* 1957;12:1158–1162.
3. Balint R, Cassidy NJ, Cartmell SH. Electrical stimulation: A novel tool for tissue engineering. *Tissue Eng B Rev* 2013;19:48–57.
4. Fredericks DC, Smucker J, Petersen EB, Bobst JA, Gan JC, Simon BJ, Glazer P. Effects of direct current electrical stimulation on gene expression of osteopromotive factors in a posterolateral spinal fusion model. *Spine* 2007;32:174–181.
5. Bodamyali T, Kanczler J, Simon B, Blake D, Stevens C. Effect of faradic products on direct current-stimulated calvarial organ culture calcium levels. *Biochem Biophys Res Commun* 1999;264:657–661.
6. Ateh DD, Navsaria HA, Vadgama P. Polypyrrole-based conducting polymers and interactions with biological tissues. *J R Soc Interface* 2006;3:741–752.
7. Marino AA, Becker RO, Soderholm SC. Origin of the piezoelectric effect in bone. *Calcif Tissue Res* 1971;8(1):177–180.
8. Hardy JG, Sukhvasi RC, Aguilar D, Villancio-Wolter MK, Mouser DJ, Geissler SA, Nguy L, Chow JK, Kaplan DL, Schmidt CE. Electrical stimulation of human mesenchymal stem cells on biomaterialized conducting polymers enhances their differentiation towards osteogenic outcomes. *J Mater Chem B* 2015;3:8059–8064.
9. Meng S, Rouabhia M, Zhang Z. Electrical stimulation modulates osteoblast proliferation and bone protein production through heparin-bioactivated conductive scaffolds. *Bioelectromagnetics* 2013;34:189–199.
10. Hronik-Tupaj M, Rice WL, Cronin-Golomb M, Kaplan DL, Georgakoudi I. Osteoblastic differentiation and stress response of

- human mesenchymal stem cells exposed to alternating current electric fields. *Biom Eng Online* 2011;10:9.
11. McLeod KJ, Donahue HJ, Levin PE, Fontaine MA, Rubin CT. Electric fields modulate bone cell function in a density-dependent manner. *J Bone Miner Res* 2009;8:977–984.
 12. Zhang J, Li M, Kang E-T, Neoh KG. Electrical stimulation of adipose-derived mesenchymal stem cells in conductive scaffolds and the roles of voltage-gated ion channels. *Acta Biomater* 2016;32:46–56.
 13. Thamsborg G, Florescu A, Oturai P, Fallentin E, Tritsarlis K, Dissing S. Treatment of knee osteoarthritis with pulsed electromagnetic fields: A randomized, double-blind, placebo-controlled study. *Osteoarthritis Cartil* 2005;13:575–581.
 14. Balint R, Cassidy NJ, Cartmell SH. Conductive polymers: Towards a smart biomaterial for tissue engineering. *Acta Biomater* 2014;10:2341–2353.
 15. Guimard NK, Gomez N, Schmidt CE. Conducting polymers in biomedical engineering. *Progr Polym Sci* 2007;32:876–921.
 16. Yu Q-Z, Shi M-M, Deng M, Wang M, Chen H-Z. Morphology and conductivity of polyaniline sub-micron fibers prepared by electrospinning. *Mater Sci Eng B* 2008;150:70–76.
 17. Prabhakaran MP, Ghasemi-Mobarakeh L, Jin G, Ramakrishna S. Electrospun conducting polymer nanofibers and electrical stimulation of nerve stem cells. *J Biosci Bioeng* 2011;112:501–507.
 18. Guo Y, Li M, Mylonakis A, Han J, MacDiarmid AG, Chen X, Lelkes PI, Wei Y. Electroactive oligoaniline-containing self-assembled monolayers for tissue engineering applications. *Biomacromolecules* 2007;8:3025–3034.
 19. Borriello A, Guarino V, Schiavo L, Alvarez-Perez MA, Ambrosio L. Optimizing PANi doped electroactive substrates as patches for the regeneration of cardiac muscle. *J Mater Sci Mater Med* 2011;22:1053–1062.
 20. Zhang Q-S, Yan Y-H, Li S-P, Feng T. Synthesis of a novel biodegradable and electroactive polyphosphazene for biomedical application. *Biomed Mater* 2009;4:
 21. Rivers TJ, Hudson TW, Schmidt CE. Synthesis of a novel, biodegradable electrically conducting polymer for biomedical applications. *Adv Funct Mater* 2002;12:33–37.
 22. Hu J, Huang L, Zhuang X, Zhang P, Lang L, Chen X, Wei Y, Jing X. Electroactive aniline pentamer cross-linking chitosan for stimulation growth of electrically sensitive cells. *Biomacromolecules* 2008;9:2637–2644.
 23. Liu Y, Hu J, Zhuang X, Zhang P, Wei Y, Wang X, Chen X. Synthesis and characterization of novel biodegradable and electroactive hydrogel based on aniline oligomer and gelatin. *Macromol Biosci* 2012;12:241–250.
 24. Zhang L, Li Y, Li L, Guo B, Ma PX. Non-cytotoxic conductive carboxymethyl-chitosan/aniline pentamer hydrogels. *React Funct Polym* 2014;82:81–88.
 25. Rinaudo M. Chitin and chitosan: Properties and applications. *Progr Polym Sci* 2006;31:603–632.
 26. Pillai CKS, Paul W, Sharma CP. Chitin and chitosan polymers: Chemistry, solubility and fiber formation. *Progr Polym Sci* 2009;34:641–678.
 27. Kast CE, Bernkop-Schnürch A. Thiolated polymers—thiomers: Development and in vitro evaluation of chitosan–thioglycolic acid conjugates. *Biomaterials* 2001;22:2345–2352.
 28. Thein-Han WW, Kitiyanant Y, Misra RDK. Chitosan as scaffold matrix for tissue engineering. *Mater Sci Technol* 2008;24:1062–1075.
 29. Di Martino A, Sittering M, Risbud MV. Chitosan: A versatile biopolymer for orthopaedic tissue-engineering. *Biomaterials* 2005;26:5983–5990.
 30. Khor E, Lim LY. Implantable applications of chitin and chitosan. *Biomaterials* 2003;24:2339–2349.
 31. Bakhshandeh B, Soleimani M, Ghaemi N, Shabani I. Effective combination of aligned nanocomposite nanofibers and human unrestricted somatic stem cells for bone tissue engineering. *Acta Pharmacol Sin* 2011;32:626–636.
 32. Kim H-W, Kim H-E, Salih V. Stimulation of osteoblast responses to biomimetic nanocomposites of gelatin–hydroxyapatite for tissue engineering scaffolds. *Biomaterials* 2005;26:5221–5230.
 33. Yamauchi K, Goda T, Takeuchi N, Einaga H, Tanabe T. Preparation of collagen/calcium phosphate multilayer sheet using enzymatic mineralization. *Biomaterials* 2004;25:5481–5489.
 34. Wei G, Ma PX. Structure and properties of nano-hydroxyapatite/polymer composite scaffolds for bone tissue engineering. *Biomaterials* 2004;25:4749–4757.
 35. Sui G, Yang X, Mei F, Hu X, Chen G, Deng X, Ryu S. Poly-L-lactic acid/hydroxyapatite hybrid membrane for bone tissue regeneration. *J Biomed Mater Res A* 2007;82:445–454.
 36. Thein-Han WW, Misra RDK. Biomimetic chitosan–nanohydroxyapatite composite scaffolds for bone tissue engineering. *Acta Biomater* 2009;5:1182–1197.
 37. Phinney DG, Prockop DJ. Concise review: Mesenchymal stem/multipotent stromal cells: The state of transdifferentiation and modes of tissue repair—Current views. *Stem Cells* 2007;25:2896–2902.
 38. Hafizi M, Bakhshandeh B, Soleimani M, Atashi A. Exploring the encephalineric differentiation potential in adult stem cells for cell therapy and drug screening implications. *In Vitro Cell Dev Biol Anim* 2012;48:562–569.
 39. Kim IS, Song JK, Song YM, Lee TH, Cho TH, Lim SS, Pan H, Kim SJ, Hwang SJ. Novel action of biphasic electric current in vitro osteogenesis of human bone marrow mesenchymal stromal cells coupled with VEGF production. *Bone* 2008;43:S43–S44.
 40. Titushkin I, Cho M. Regulation of cell cytoskeleton and membrane mechanics by electric field: Role of linker proteins. *Biophys J* 2009;96:717–728.
 41. Sun S, Titushkin I, Cho M. Regulation of mesenchymal stem cell adhesion and orientation in 3D collagen scaffold by electrical stimulus. *Bioelectrochemistry* 2006;69:133–141.
 42. Liu Y, Cui H, Zhuang X, Wei Y, Chen X. Electrospinning of aniline pentamer-graft-gelatin/PLLA nanofibers for bone tissue engineering. *Acta Biomater* 2014;10:5074–5080.
 43. Hu J, Huang L, Zhuang X, Chen X, Wei Y, Jing X. A new oxidation state of aniline pentamer observed in water-soluble electroactive oligoaniline-chitosan polymer. *J Polym Sci A Polym Chem* 2008;46:1124–1135.
 44. Behnia H, Khojasteh A, Soleimani M, Tehrani A, Khoshzaban A, Keshel SH, Atashi R. Secondary repair of alveolar clefts using human mesenchymal stem cells. *Oral Surg Oral Med Oral Pathol Oral Radiol Endodontol* 2009;108:e1.
 45. Zhang H, Zong R, Zhu Y. Photocorrosion inhibition and photoactivity enhancement for zinc oxide via hybridization with monolayer polyaniline. *J Phys Chem C* 2009;113:4605–4611.
 46. Cao J, Man Y, Li L. Electrical stimuli improve osteogenic differentiation mediated by aniline pentamer and PLGA nanocomposites. *Biomed Rep* 2013;1:428–432.
 47. Mohammadi Amirabad L, Massumi M, Shamsara M, Shabani I, Amari A, Mossahebi Mohammadi M, Hosseinzadeh S, Vakilian S, Steinbach SK, Khorramizadeh MR, Soleimani M, Barzin J. Enhanced cardiac differentiation of human cardiovascular disease patient-specific induced pluripotent stem cells by applying unidirectional electrical pulses using aligned electroactive nanofibrous scaffolds. *ACS Appl Mater Interfaces* 2017;9:6849–6864.
 48. Tandon N, Marsano A, Maidhof R, Wan L, Park H, Vunjak-Novakovic G. Optimization of electrical stimulation parameters for cardiac tissue engineering. *J Tissue Eng Regen Med* 2011;5:e115–e125.
 49. Hu WW, Hsu YT, Cheng YC, Li C, Ruaan RC, Chien CC, Chung CA, Tsao CW. Electrical stimulation to promote osteogenesis using conductive polypyrrole films. *Mater Sci Eng C Mater Biol Appl* 2014;37:28–36.
 50. McLeod KJ, Rubin CT. The effect of low-frequency electrical fields on osteogenesis. *J Bone Joint Surg Am* 1992;74:920–929.
 51. Ma X, Ge J, Li Y, Guo B, Ma PX. Nanofibrous electroactive scaffolds from a chitosan-grafted-aniline tetramer by electrospinning for tissue engineering. *RSC Adv* 2014;4:13652–13661.
 52. Duan B, Dong C, Yuan X, Yao K. Electrospinning of chitosan solutions in acetic acid with poly (ethylene oxide). *J Biomater Sci Polym Ed* 2004;15:797–811.
 53. Li L, Hsieh Y-L. Chitosan bicomponent nanofibers and nanoporous fibers. *Carbohydr Res* 2006;341:374–381.
 54. Pakravan M, Heuzey M-C, Aiji A. A fundamental study of chitosan/PEO electrospinning. *Polymer* 2011;52:4813–4824.
 55. Engler AJ, Sen S, Sweeney HL, Discher DE. Matrix elasticity directs stem cell lineage specification. *Cell* 2006;126:677–689.

56. Zhang Y, Zhang M. Synthesis and characterization of macroporous chitosan/calcium phosphate composite scaffolds for tissue engineering. *J Biomed Mater Res* 2001;55:304–312.
57. Peng H, Yin Z, Liu H, Chen X, Feng B, Yuan H, Su B, Ouyang H, Zhang Y. Electrospun biomimetic scaffold of hydroxyapatite/chitosan supports enhanced osteogenic differentiation of mMSCs. *Nanotechnology* 2012;23:485102.
58. Tsai MT, Li WJ, Tuan RS, Chang WH. Modulation of osteogenesis in human mesenchymal stem cells by specific pulsed electromagnetic field stimulation. *J Orthopaed Res* 2009;27:1169–1174.
59. Wutticharoenmongkol P, Pavasant P, Supaphol P. Osteoblastic phenotype expression of MC3T3-E1 cultured on electrospun polycaprolactone fiber mats filled with hydroxyapatite nanoparticles. *Biomacromolecules* 2007;8:2602–2610.
60. Venugopal J, Low S, Choon AT, Kumar TSS, Ramakrishna S. Mineralization of osteoblasts with electrospun collagen/hydroxyapatite nanofibers. *J Mater Sci Mater Med* 2008;19:2039–2046.
61. Lao L, Wang Y, Zhu Y, Zhang Y, Gao C. Poly (lactide-co-glycolide)/hydroxyapatite nanofibrous scaffolds fabricated by electrospinning for bone tissue engineering. *J Mater Sci Mater Med* 2011;22:1873–1884.
62. Hughes FJ, Turner W, Belibasakis G, Martuscelli G. Effects of growth factors and cytokines on osteoblast differentiation. *Periodontol* 2000 2006;41:48–72.
63. Westrin M, Xie M, Olderøy MØ, Sikorski P, Strand BL, Standal T, Papaccio G. Osteogenic differentiation of human mesenchymal stem cells in mineralized alginate matrices. *PLoS One* 2015;10:e0120374.
64. Tsao YT, Huang YJ, Wu HH, Liu YA, Liu YS, Lee OK. Osteocalcin mediates biomineralization during osteogenic maturation in human mesenchymal stromal cells. *Int J Mol Sci* 2017;18:159.
65. Chen G, Deng C, Li YP. TGF-beta and BMP signaling in osteoblast differentiation and bone formation. *Int J Biol Sci* 2012;8:272–288.
66. Bakhshandeh B, Soleimani M, Hafizi M, Paylakhi SH, Ghaemi N. MicroRNA signature associated with osteogenic lineage commitment. *Mol Biol Rep* 2012;39:7569–7581.
67. Bakhshandeh B, Hafizi M, Ghaemi N, Soleimani M. Down-regulation of miRNA-221 triggers osteogenic differentiation in human stem cells. *Biotechnol Lett* 2012;34:1579–1587.